

Compliant universal grippers as adaptive feet in legged robots

S. Hauser, M. Mutlu, P. Banzet & A.J. Ijspeert

To cite this article: S. Hauser, M. Mutlu, P. Banzet & A.J. Ijspeert (2018): Compliant universal grippers as adaptive feet in legged robots, *Advanced Robotics*, DOI: [10.1080/01691864.2018.1496851](https://doi.org/10.1080/01691864.2018.1496851)

To link to this article: <https://doi.org/10.1080/01691864.2018.1496851>

 View supplementary material 

 Published online: 27 Jul 2018.

 Submit your article to this journal 

 Article views: 26

 View Crossmark data 

Compliant universal grippers as adaptive feet in legged robots

S. Hauser ^a, M. Mutlu ^{a,b}, P. Banzet^a and A.J. Ijspeert ^a

^aBioRob, School of Engineering, EPFL, Lausanne, Switzerland; ^bVislab, Institute of Systems and Robotics, IST, Lisbon, Portugal

ABSTRACT

This work investigates the usage of compliant universal grippers as a novel foot design for legged locomotion. The method of jamming of granular media in the universal grippers is characterized by having two distinct states: a soft, fluid-like state which in locomotion can be used to damp impact forces and enable passive shape adaptation especially on rough terrain, and a hard, solid-like state that is more suited to transmit propulsion forces. We propose a system that actively uses and switches between both states of a foot design based on granular jamming and detail the implementation on a quadruped robotic platform. The mechanism is inspired by the stiffness varying function of the *tarsal bones* in a human foot, and our aim is to understand how the change of foot stiffness can be used to improve the locomotion performance of legged robots. Using the same open loop trot gait in all experiments, it is shown that a fast state transition enables the robot to profit from both states, leading to more uniform foot placement patterns also on rough terrain compared to other tested feet. This results in overall faster gaits and even enables the robot to climb steeper inclined surfaces.

ARTICLE HISTORY

Received 6 December 2017
Revised 12 April 2018
Accepted 17 May 2018

KEYWORDS

Adaptive feet; jamming;
universal gripper;
locomotion; legged robots

1. Introduction

In nature, paw-pads of, for example, dogs show a remarkable adaptability that allow them to deal with a variety of terrains. In contrast, the feet of multi-legged robots often are half-sphere-shaped or cylindrically shaped out of different materials (e.g. [1–7]). This design usually allows the simplification of an otherwise complex contact area to a single point, which in turn is used to handle advanced control strategies in closed-loop control. This is especially important in locomotion on uneven/rough terrain. Impressive locomotion capabilities have been demonstrated with this strategy in the respective research. In many cases, the centralized-control-approach usually requires three key ingredients: (i) precise force sensing that accurately measure the ground reaction forces, (ii) precise tracking of joint angle trajectories by the mechatronic system of the robot to execute a planned trajectory and (iii) relatively high computational power to collect all the sensor data, process them and plan the foot trajectories. On the one hand, these requirements can make the application of such a control system to legged robots infeasible due to their large expenses. On the other hand, even though such systems are able to perform well in certain conditions, the results do not necessarily represent animal-like behavior. Partly due to the feet's inability to adapt, in such systems the roughness of the terrain has

to be individually dealt with on a computational level through constantly changing trajectories which rather deteriorates the performance of a robot. Thus, mechanical adaptability in the feet could have the potential to reduce the need for complex control by offloading terrain adaptation from the main computational unit to the feet and hence simplifying the control. However, the design of adaptive feet for legged robots on rough terrain remains a challenge. One available strategy is to increase the number of contact points per foot (as opposed to only one contact point in the case of 'rigid' spherical feet) by, for example, splitting the foot into independent sections and let each contact point form ground contact individually. This distributes the roughness to multiple points where the final orientation of the foot is determined by an averaged influence of each point [8–10]. Other works focused in replicating the main features of human feet [11–14] and animal feet [15, 16].

Interestingly, some of the research presented is arguably focused on *avoiding* the unevenness of the terrain by creating multiple contact points. Our proposition is that creating an actual contact *area* is more beneficial for the locomotion performance as such an area may actively use the features of the ground (which may be unfavorable for a few contact points or not covered at all) for improved friction and propulsion, thus *seeking*

CONTACT S. Hauser  simon.hauser@epfl.ch

 Supplemental data for this article can be accessed <https://doi.org/10.1080/01691864.2018.1496851>

unevenness. Additionally, the weight of a robot is more evenly distributed over a contact area rather than focused on contact points, potentially allowing the robot to also locomote on soft grounds (e.g. sand or snow). Intuitively, it is clear that a spatial conformation of the foot to uneven terrain requires compliance, and thus a soft foot seems desirable. However, as it is described in [17] and further analyzed in [12], a purely soft foot creates new issues. A compliance below a critical level is not anymore able to stabilize the system as the support polygon is not static; applying a required force within the support polygon to compensate a slight shift of the center of gravity of the robot gets absorbed by the compliance, resulting in the robot falling. Moreover, propulsion forces orthogonal to the contact area get absorbed as well. Instead of pushing a robot forward, the movement of, for example, a step will simply exchange energy with the compliance without resulting in a net forward motion. A compromise seems unavoidable – a foot should be soft enough to adapt and stiff enough to allow propulsion.

One possibility to deal with this dilemma is to separate two distinct actions of a foot during stance phase. First, the foot must adapt to the uneven terrain and damp the impact of the foot on the ground to ensure an undisturbed ground contact without slipping and bouncing. Then, it must use the shear forces transmittable in the contact area to create the necessary propulsion forces. As discussed above, these two actions seem to be somewhat opposite to each other. While adaptation and damping requires a certain softness in the system, controlled force transmission prefers a stiff system. A possible class of design methods that can offer such mechanical state-changes are *variable stiffness mechanisms*. Indeed, the research in [17] states the importance of state-switching and employs a clever mechanism in the foot that passively achieves the state transition using the weight of the robot. Their developed foot consists of four separate fingers that are unconstrained at touchdown to enable the terrain adaptation (the research does not mention damping). The weight of the robot then engages a brake (interestingly related to the principle of jamming that is discussed below) that locks the finger arrangement in place to perform locomotion. Although the work is motivated by developing a ‘sole’ that enlarges the support polygon of the robot during stance, the mechanism creates four contact points per foot without creating an actual contact area – as in animal feet – that could interact as a whole with the structure of the terrain.

In the case of a dog paw, we hypothesize that the adaptive capabilities of the aforementioned paw-pads stems from a complex, local interplay of bones, tissues and muscles which is able to form a contact area that can smoothly transition between soft and hard states. As a result, this

leads to extremely versatile locomotion capabilities [18], although the mechanisms are not yet fully understood. In humans, recent research indicates how the transition could function. The bones and muscles together with the surrounding tissue form an inherently compliant structure which can act as a damper at touchdown. A group of bones known as the *tarsal bones* near the end of the tibia has the ability to change its structural rigidity from flexible to rigid through a rotation of the foot, rearranging these bones in such a way that an interlocked structure is formed. The rotation happens passively during stance phase and is assisted by the contraction of the muscles in the foot that keep the bones in their interlocked arrangement. This allows the propulsion force transmission to the ground until takeoff when the foot becomes compliant again [19, 20].

The goal of this work is to understand how a change of foot stiffness can be used to improve the locomotion performance of legged robots, for which we abstract the mechanism and design and implement it in a quadruped robot. The abstraction aims at simplifying the mechanical construction as a replication of the complex anatomy would be too challenging. In this research, we use the jamming of granular media as the enabling technology as it offers the possibility of state-switching. Granular media behave fluid-like in open space and solid-like in confined (jammed) space [21], and this property has led to a number of applications (e.g. grippers [22], dampers [23] and actuators [24]). Further, it is worth mentioning that in [20] the unlocked configuration of the tarsal bones is described as ‘a loose bag of bones’, unconsciously hinting at the idea to approximate the structure with macroscopic granules. The feasibility of such a foot design has already been investigated in [25], however without the state-switch of the granular media. Nevertheless, it has been shown that jamming membranes possess beneficial damping properties in their soft state and are able to apply sufficient propulsion forces in their jammed state. A more in-depth analysis of the effects of state-switching a jamming membrane on the ground reaction forces can be found in [26] where a jamming membrane drops onto a structured terrain in its soft state and upon impact rapidly (in approx. 60 ms) switches to its hard state. In comparison to a previously used rubber foot and a non-switching jamming membrane, the switching membrane inherits the beneficial damping properties of the soft state, which avoids bouncing and quickly creates an undisturbed ground contact. Further, it is able to transmit the locomotion forces immediately after the damping period by the rapid state-switch, resulting in the maximal shear force transmission in 30% of the time needed for the same force transmission with the rubber foot.

These aspects are promising for the application of fast state-switching jamming membranes to legged locomotion, especially in rough terrain where damping and shape adaptation potentially play a key role in locomotion performance and balance. Further, due to their initial development as universal grippers, jamming membranes can offer a multi-functional use as feet in locomotion and grippers for manipulation.

2. Methods

The numerical simulation of compliant, shape-changing objects is a difficult problem to tackle and moreover likely suffers largely from the reality gap. As our aim is to understand how legged animals could use a change in foot stiffness during locomotion with the help of real robots, we decided to conduct this experimental study in hardware only, and this section explains all the used hardware in detail: the robotic platform, the pump and valve system, the jamming membranes as feet, the on-board and off-board sensors, the control of the main body and the evacuation system and the terrain.

2.1. Robotic platform

2.1.1. Foot design

The foot design is based on the end effector design in [27] with similar dimension as in [26]. A latex balloon with a diameter of approximately 3.5 cm is filled with cubic rubber granules with a side length of 4 mm (Neukadur Prototflex HS 75). The open end of the balloon is clamped between a disk and a lid that form an airtight seal where each foot is connected by a tube to the pump-valve-system (Figure 1(a)). The reasons to use compliant cubes as granules instead of, for example, ground coffee are threefold. First, it has been shown by [28] that cubic granules perform a *geometrical* jamming due to their shape, which enables jamming with less pressure difference. This results in less demanding specifications for the

pump, i.e. a smaller, lighter pump which could prove beneficial for such a mobile jamming application. Second, the same research and [27] show that these compliant granules have the ability to change the overall stiffness of the membrane linearly with the applied vacuum pressure. Even though evacuation to different vacuum pressure levels has not been implemented in this work, a change in membrane stiffness could become important especially in different gait patterns and higher frequencies. Third, bigger granules result in less memory effect which occurs by the pack of granules sustaining the shape adaptation even after the deformation of the membrane. Resetting the granules to their initial, unpacked arrangement can be achieved by a burst of positive pressure (e.g. [29]) which would require a separate positive pressure reservoir. In order to keep the evacuation system as light as possible, only a vacuum reservoir has been implemented, and the membrane reset to only atmospheric pressure showed a sufficient mitigation of the memory effect.

2.1.2. Main body

The main body of the robot is largely based on the design in [30] where this robot was used to investigate a local feedback mechanism for active stabilization. A rectangular, wooden plate holds all components and four legs are attached on its edges. Each leg consists of two servo motors for hip (Dynamixel RX-28, 18 V) and knee joint (Dynamixel AX-12A, 12 V) that are connected in series such that their movement is in the sagittal plane. The dimensions of the body are 28 cm x 41 cm and the length of each leg (with the foot) is 23 cm. The total weight of the robot is 30 N (Figure 2 left).

2.1.3. Evacuation system

Even though a mechanism for fast evacuation of a single foot based on a closed-air solenoid and syringe system has been implemented in [26], the system had to be modified because the same mechanism was not scalable for a mobile quadruped. Hence, another system with

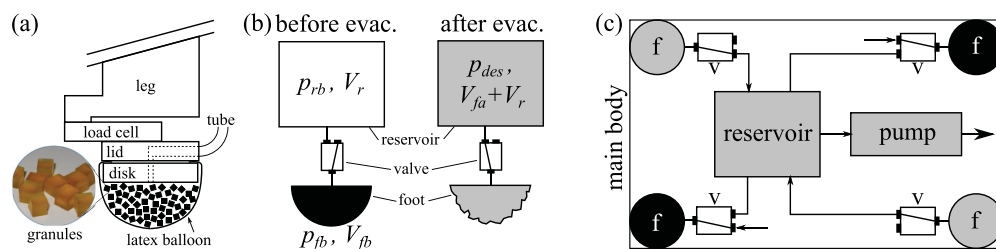


Figure 1. Schematics of the system. (a) A latex balloon is filled with cubic rubber granules and clamped between a disk and a lid to which a tube is connected. A load cell between the foot and the leg measures the vertical load on each leg (front view of the foot). (b) The two systems ‘reservoir’ and ‘foot’, first separated before evacuation and then in the combined configuration after evacuation. (c) Four feet (f) are each connected to a valve (v) which redirects the airflow to either the outside atmosphere (for a walking trot gait, e.g. the bottom left and top right foot) or to the central vacuum reservoir (top left and bottom right foot) in which a vacuum is created by a continuously running pump (view from below).

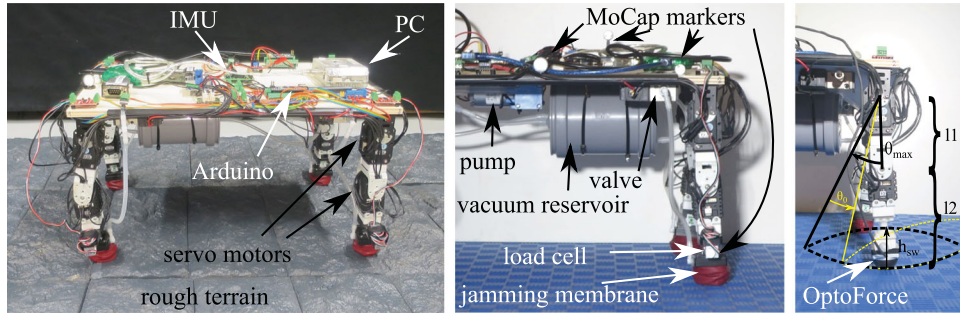


Figure 2. The robotic platform. Left: The quadruped robot standing on the used rough terrain. A main body frame holds an embedded PC (Odroid), IMU and the separate evacuation control unit. Four legs are fixed on each edge, consisting each of two servo motors in series (hip and knee) and the foot. Middle: The pump, vacuum reservoir and valves are fixed underneath the main frame. The evacuation of each foot is triggered by a load cell mounted directly on top of the jamming membrane. Right: Configuration of the leg with an OptoForce (OF) sensor as the foot and parameters of the trajectory.

a reservoir and valves has been developed. A vacuum pump continuously evacuates a single reservoir volume formed by a PCV pipe to which each foot is connected over a separate valve. The valve normally directs the air flow of a foot to atmospheric pressure (soft state). When triggered by a load cell, the valve connects the airflow of a foot to the vacuum reservoir, causing the foot to evacuate to the level of vacuum pressure inside the reservoir (hardened state). These switches are activated depending on the stance and swing phase of each leg individually, described in Section 2.3.2.

When dimensioning the pump-valve system, two main aspects were taken into consideration: the required vacuum pressure level and the speed of the evacuation, both defining the performance of the pump, the size of the reservoir and the specifications of the valves. Additionally, the system should be as light as possible to be able to be integrated in a mobile quadruped robot. For the specific requirements, it has been shown in [25] that a pressure difference of -180 mbar in the jamming membrane versus atmospheric pressure produces a significant effect on the locomotion performance, hence the desired pressure difference was around -200 mbar. Further, [26] shows that an evacuation speed of around 60 ms is needed to enable the advantages of state-switching. In order to find the performance requirements for the mechatronic components, we define two separate systems, one foot and the reservoir, at two different states – before evacuation and after evacuation – and consider that the pump is switched off in both states (Figure 1(b)). Since this action only requires the valve to open, it is clear that the total mass of the air during this process stays unchanged, i.e.

$$n_{fb} + n_{rb} = n_{fa} + n_{ra} \quad (1)$$

where n_{fb} is the number of moles of air in the foot before evacuation, n_{fa} is the number of moles of air in

the foot after evacuation, and analogue for the moles in the reservoir n_{rb} and n_{ra} . By considering air as an ideal gas and constant temperature, we can substitute Boyle’s law into each component of Equation (1), solve for the unknown pressure inside the reservoir before evacuation and obtain

$$p_{rb} = p_{des} \cdot \frac{V_{fa} + V_r}{V_r} - \frac{p_{fb} \cdot V_{fb}}{V_r} \quad (2)$$

where p_{rb} is the required pressure in the reservoir before evacuation in (mbar), p_{des} the desired final vacuum pressure in (mbar), V_r the constant volume of the reservoir in (mL), p_{fb} the pressure in the foot before evacuation in (mbar), V_{fb} the air volume in the foot before evacuation in (mL) and V_{fa} the air volume in the foot after evacuation in (mL). Equation (2) describes an inversely proportional relationship between the volume of the reservoir and the initial vacuum in the reservoir before evacuation of the foot, i.e. a larger reservoir puts the required initial vacuum pressure closer to the final desired pressure which in turn reduces the power requirements of the pump. In our case, we define $p_{des} = 800$ mbar, $p_{fb} \approx 1000$ mbar at atmospheric pressure and $V_{fb} \approx 10$ mL. A PVC vacuum reservoir of 500 mL seemed feasible both in size and weight. Since the soft foot deforms under the vacuum, V_{fa} will be only a fraction of V_{fb} and thus around two orders of magnitude smaller than V_r . In Equation (2), we therefore neglected the contribution of V_{fa} which simplifies the first term to p_{des} , resulting in a required pressure of $p_{rb} = 780$ mbar. Next, we need to find a vacuum pump with the appropriate airflow at this vacuum pressure level, i.e. a vacuum pump must be able to evacuate the air volume of the foot within a required time. By again using Boyle’s law in Equation (3), we find that the foot volume V_{fb} of 10 mL at $p_{fb} = 1000$ mbar equals a volume V_{eq} of 12.8 mL at $p_{rb} = 780$ mbar by

setting

$$V_{eq} = \frac{P_{fb} \cdot V_{fb}}{P_{rb}} \quad (3)$$

This only represents the evacuation volume of one foot. The real robot with four feet connected to the reservoir (Figure 1(c)) was designed to have a gait cycle of maximum 1 Hz, meaning that there are at most four evacuation events per second. This results in an airflow of $4 \cdot 12.8 \text{ mL/s} = 3072 \text{ mL/min}$ at 780 mbar. Small-scale diaphragm pumps offer the possibility to reach relatively high levels of vacuum pressure suitable for the present system, hence by taking some performance losses due to for example tubing into account, a stronger, relatively lightweight diaphragm pump with the appropriate specifications has been used (Parker D743-21-01, parallel airflow of $\approx 3300 \text{ mL/min}$ at 780 mbar). Concerning the tubes, it has been demonstrated in [26] that silicone tube with an inside diameter of 3 mm is wide enough to enable the evacuation in 60 ms, thus the same tube was used. At last, the same airflow and pressure requirements also apply to the valves used for each foot (SMC VK332W-6DO-M5-Q). Both pump and valves run on 12 V which is already available on the robotic platform. The pump, valves, reservoir and feet altogether weight roughly 10 N (i.e. one-third of the total body mass).

2.2. Sensors

A variety of on-board and off-board sensors are integrated in the system, both for measuring locomotion parameters and controlling the robot. On-board are encoders in each servo motor, an IMU (Xsens MTi-3 AHRS) measuring roll, pitch and yaw angles as well as acceleration in x -, y - and z -direction. Additionally, each leg is equipped with a load cell (CZL635 0–5 kg) that – with a separate Arduino Nano – measures the load on each leg (Figure 1(a)). This information is used by the evacuation controller to distinguish stance and swing phase of each leg. The Arduino also reads a pressure sensor (Honeywell 030PAAA5) connected to the fore left foot to measure the evacuation speed and the reached vacuum pressure level (Figure 2 middle). Further, a Motion-Capture system (MoCap) system provides off-board position and orientation data of the trunk of the robot as well as the position of the lid of the fore right foot.

All the on-board sensors are connected via USB and the off-board sensors via WiFi to an embedded on-board PC (Odroid-XU4) that controls the servo motors and logs all sensor data. The evacuation system of the feet however is designed to be a standalone control unit that can be switched on and off separately and shares no communication with the main PC besides the logging.

2.3. Control

2.3.1. Foot trajectory

The foot trajectory is the same as in [30] which has been obtained by a particle swarm optimization of swing amplitude θ_{max} , swing height h_{sw} and locomotion speed. The trajectory controller employs an oscillator in each leg that moves each foot back and forth in an elliptical fashion with a swing amplitude of $\theta_{max} = 0.3$ rad and swing height of $h_{sw} = 1.5$ cm in position control. The dimensions of the lengths of the upper thigh l_1 and the lower thigh l_2 have been updated to $l_1 = 79$ mm and $l_2 = 110$ mm. The control is kept open loop and the phase lag of the legs are chosen such that the robot performs the same trotting gait for all experiments. For the gaits involving an inclined surface, the trajectory has been rotated backwards around the hip joint by $\theta_0 = 0.1$ rad (see Figure 2 right for details) to shift the center of gravity slightly forward to assist the climbing up movement. Due to bandwidth limitations of the servo motors, a gait frequency of 0.5 Hz is selected for all experiments.

2.3.2. Jamming membrane state-switch

The evacuation is controlled by the separate Arduino that processes the data from each load cell in a binary fashion: as soon as a load cell detects the touchdown of a foot, the valve of that foot gets activated which leads to the evacuation of the foot. Once the leg is determined to be in swing phase, the valve deactivates which makes the foot reset to atmospheric pressure. It is important to notice that this control is local only and acts on each foot individually, regardless of the state of the respective leg or the other legs.

2.4. Terrain

The terrain selection is guided by the hypotheses that (1) the jamming membranes improve friction and damping properties and also influence the overall balance of the robot and (2) the shape adaptation and state-switch of the jamming membranes enables the robot to locomote faster on rough terrain and climb steeper slopes. Hence, a flat smooth ground is used to form a baseline, however the majority of the experiments are performed on rough terrain. The terrain consists of a series of bricks fixed on a wooden panel of 0.8 m width and 3 m length. The bricks form a landscape of continuous roughness as well as discrete transitions between the bricks. Figure 2 (left) shows the roughness of the terrain in comparison to the robot. This terrain is used in the three configurations flat, inclined by 3 degrees and inclined by 5 degrees.

3. Experiments

3.1. Evacuation speed

The first experiment was designed to validate the performance of the evacuation system. The robot is initialized to its trot gait and put on flat, smooth ground after the full vacuum in the reservoir has been generated by the pump. The pressure sensor is measuring the pressure in the fore left foot. The trigger to the valve that evacuates this foot is set to activate as soon as its load cell bears more than 3 N during stance phase which represents 10% of the robot's weight. The pressure and load are measured for seven walking cycles and for each cycle, the time between triggering the stance phase and reaching the maximal vacuum pressure level in the foot is calculated as well as triggering the swing phase and the time to reset the foot.

3.2. Altering ground reaction forces

After the successful validation of the evacuation system, the altering of ground reaction forces was investigated to test the improvement of friction and damping properties in hypothesis (1). As described earlier, the jamming membrane is thought to act in two stages: it first damps vertical impact forces of the touchdown in its soft state and enables shape adaptation, which is expected to lead to a faster undisturbed contact between the membrane and the terrain, and then transmits horizontal propulsion forces after the state-switch to the hardened state. To exploit the full advantages of this state-switch, it is clear that it should transfer the physical characteristics of the membrane from the best case for damping and shape adaptation to the best case for force transmission. As described earlier, we may not achieve the best force transmission configuration as we only investigate one solid-like state given by the performance of the evacuation system. This only creates a more suitable condition for controlled force transmission but not necessarily represents the best case; more experiments in further studies are needed to move towards optimality. However, for the damping and shape adaptation configuration, the best case is when the granules are able to flow under atmospheric pressure. It is shown in [27] and [25] that any negative pressure difference in the membrane changes the spring characteristics and thus bounciness, deteriorating the damping capabilities. Additionally, unconstrained shape adaptation requires the granules to be in their unjammed state which is the case when no pressure difference between the surrounding atmosphere and the inside of the membrane is present. These considerations lead to the rationales that for our experiments, (i) the state-switch is necessary as it is the enabling method to modify the physical characteristics of the foot which

is the basis for our hypotheses and (ii) the state-switch occurs from atmospheric pressure to the pressure difference given by the evacuation system to produce the maximal modification in these physical characteristics.

Even though it is intuitive that the state-switch should happen as quickly as possible, it could be beneficial to delay the switch, especially not to weaken the damping phase (e.g. the membrane is hard before the impact is fully damped which would prevent the maximal damping effect). Thus, drop tests similar to [26] have been performed with different delays. A jamming membrane with its load cell is fixed on a hinge that restricts the movement to only let the membrane fall vertically onto a horizontally moving force plate from a height of 1.5 cm (maximal height of the stance phase). The foot is weighted such that the steady-state vertical gravitational force corresponds to one quarter of the robot's weight (7.5 N). A treadmill moves the force plate horizontally with 8.3 cm/s (0.3 km/h), which is comparable to the tested maximal speed of the robot with the jamming membrane feet (9.6 cm/s). The membrane is then dropped onto the force plate which records the vertical and horizontal forces during and after touchdown at 10,000 Hz. Figure 3 shows the setup of the drop test experiments. The drops were also recorded with a high-speed camera at 960 fps. The time between the detection of ground contact by the load cell and the activation of the evacuation valve is varied between 0, 25, 50 and 75 ms. For each configuration, three trials were recorded and smoothed with a moving average filter with a window size of 10 and equal weights. Then, the mean and standard deviation is calculated with the curves synchronized to the time of the maximal force of the first impact force peak. Additionally, the results are compared to the previously used OptoForce sensors as well as the jamming membrane under only atmospheric pressure (soft state) and full vacuum pressure (hardened state), respectively.

3.3. Locomotion performance

At last, the locomotion performance of the robot with the jamming membranes as feet is analyzed. To test the shape adaptation and locomotion performance in hypothesis (2), locomotion is performed on four different terrain layouts: (i) flat, smooth ground, (ii) flat, rough terrain, (iii) rough terrain with an inclination of 3 degrees and (iv) rough terrain with an inclination of 5 degrees. On each of these layouts, the locomotion performance is compared in four different foot configurations: (i) OptoForce sensors (OF), (ii) jamming membranes with state-switch (JMSS, 0 ms delay), (iii) jamming membranes in atmospheric pressure (JMA) and (iv) jamming membranes in their vacuumed state only (JMV). For each run, the robot

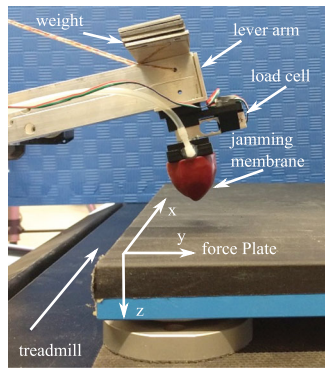


Figure 3. Setup of the drop test experiments. A hinge drops the attached weighted foot from a height of 1.5 cm onto a horizontally moving force plate which measures vertical and horizontal ground reaction forces. Drops were performed with an OF sensor, jamming membranes with varying evacuation delays (0, 25, 50 and 75 ms) as well as under atmospheric pressure and full vacuum pressure, respectively.

was first ensured to be in a steady-state locomotion pattern. Then, 10 consecutive walking cycles are recorded which includes IMU data, tracking of the main body frame and tracking of the fore left foot.

4. Results and discussion

4.1. Evacuation speed

In Figure 4, the vacuum pressure of the fore left foot is shown for one gait cycle together with the load cell measurement of the foot. Although the system was designed to achieve a pressure difference of around -200 mbar, Figure 4 shows that a pressure difference of around -500 mbar is reached. This can be explained with the slower gait frequency of 0.5 Hz instead of 1 Hz. This effectively halves the required airflow from 3072 mL/min at 780 mbar absolute pressure to around 1500 mL/min which the pump is still able to deliver at 600 mbar absolute pressure. Considering an overestimation of the foot volume, the airflow likely is even lower, dropping the final pressure to 500 mbar absolute pressure. The larger pressure difference could question the reported observations made for the smaller pressure difference in [25]. However, instead of adjusting the mechatronic components to achieve the weaker -200 mbar difference, we speculated that the qualitative aspects of the state-switch (namely to trade damping and adaptation capabilities for force transmissibility) still hold true, and may even be more pronounced with the higher pressure difference. Nevertheless, the system is potentially over-performing and could be designed with lighter and less power-consuming components, especially a less powerful pump which is

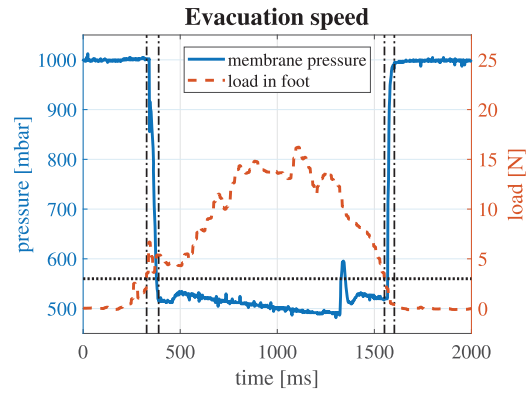


Figure 4. Pressure and load cell measurements of the fore left foot during one gait cycle. After the load cell triggers the evacuation at 3 N (dotted horizontal line), it takes approximately 61 ms for the foot to reach a pressure difference of -500 mbar (black vertical lines on the left). The leg supports up to half of the total body mass during stance phase and triggers the membrane reset to atmospheric pressure again at 3 N; the reset takes approximately 48 ms (black vertical lines on the right).

the main reason for the higher pressure difference. Moreover, we did not investigate the optimal pressure difference; our experiments with this type of membrane and granules however suggest that a wide range of pressure difference is able to create the desired effect of state-switching, potentially with varying characteristics which may be useful for gait-dependent stiffness adaptation. In any case, even the larger pressure difference is achieved in 61 ± 3.8 ms from the time that the load cell triggers the evacuation, and the evacuation itself takes only 49 ± 4.1 ms. This was considered well within the desired characteristics. Further, even though no active inflation process is implemented, the membrane reset to atmospheric pressure after the trigger takes only 47.7 ± 4.4 ms (where the actual inflation takes 31.9 ± 4.9 ms). Concerning the load, it can be seen that a trigger of 3 N (10% of the total body mass of 30 N) is appropriate to avoid false triggers due to noise. Further, the leg typically supports 15 N during the stance phase which is the moment where the total body mass is supported by two legs only, resulting in each leg bearing half of the total load. No significant force peaks due to impacts and dynamical effects are visible.

4.2. Altering ground reaction forces

The force measurements of the drop tests are displayed in Figure 5. Each graph shows the mean and standard deviation of the three trials performed. For each configuration, the motion of the foot undergoes different phases. At first, depending on the damping capabilities, bouncing may occur in which the vertical force recordings show a declining force peak pattern. During this period, the

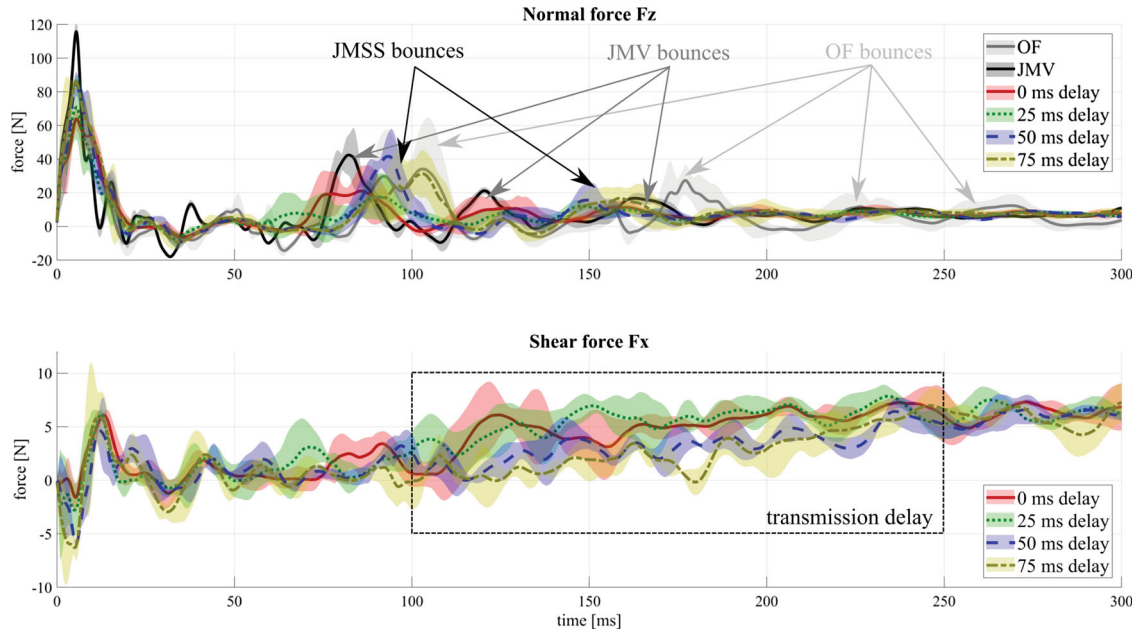


Figure 5. Force measurements of the drop tests, each graph shows the mean (bold) and standard deviation (shaded area) of three trials. Top: Vertical impact forces. OF and JMV bounce off the ground several times, delaying the transmission of horizontal propulsion forces. The jamming membranes possess an improved damping, however different evacuation delays in the jamming membranes does not significantly alter the damping behavior. Bottom: Horizontal propulsion forces (OF and JMF are omitted for clarity). A shorter evacuation delay has a tendency to a faster shear force transmission (e.g. between 100 and 250 ms), thus the shortest evacuation delay of 0 ms has been chosen for the locomotion experiments.

horizontal forces onto the moving ground are stochastically around zero as no proper ground contact has been formed yet. Only after the foot comes close to a rest in vertical motion, it is able to cause a gradual increase in the horizontal forces. All configurations then end in a steady-state sliding motion with comparable forces in both horizontal and vertical directions. The two main criteria for selecting the best foot configuration are the damping behavior and the propulsion delay where we are aiming at the fastest impact damping and shortest propulsion delay. The top graph in Figure 5 focuses on the damping of the vertical impact (normal) forces. It can be seen that the OF sensor possesses poor damping capabilities which is manifested in several bounces after the initial touchdown. This is an undesired effect as it delays the transmission of the horizontal propulsion forces which is expected to reduce the locomotion speed. For the jamming membrane under full vacuum (JMV), the bouncy behavior is less pronounced with three peaks that can be distinguished after the initial touchdown. Additionally, the fully jammed membrane results in the overall stiffest configuration. This is visible in the force peak of the first touchdown which is higher and shorter than in the other configurations, as well in the higher bouncing frequency, indicating inferior damping capabilities. At last, the best damping characteristics are shown by the state-switching jamming membranes which display at most two rebounds. For the state-switching jamming

membranes with different delays, no significant observation could be made as they all show a similar damping behavior. The influence of the delay is more visible in the bottom graph of Figure 5 where horizontal propulsion forces are visible for the different configurations. OF and JMV are excluded and omitted for visibility reasons and due to their inferior damping characteristics and only the state-switching jamming membrane cases are shown (JMSS). A tendency for later shear force transmission with increasing evacuation delays is visible, for example between 100 and 250 ms the cases with a shorter delay already transmit higher shear forces. This trend together with the observation about the similar damping behavior above led to the selection of the case with the shortest delay possible, i.e. the jamming membrane with 0 ms evacuation delay has been chosen for all following experiments.

4.3. Locomotion performance

The collected tracking data is split into two metrics. The tracking of the main body of the robot is converted into a global speed v (cm/s) by calculating the overall difference in forward motion Δx in (cm) over the duration of 10 cycles (= 20 seconds), i.e. $v(\text{cm/s}) = \Delta x(\text{cm})/20(\text{s})$. The respective speed for each tested configuration is indicated in Table 1. It can be seen that the OF sensors outperform the other feet on the flat, smooth terrain.

Table 1. Speed comparison on different terrains. While OF has the fastest locomotion on flat, smooth terrain, the state-switching jamming membrane outperforms all other foot configurations on rough terrain and is even able to climb a 5 degree inclined slope.

Terrain	Foot	Speed v (cm/s)
flat	OptoForce (OF)	12.1
	JM state-switch (JMSS)	9.6
	JM atmospheric (JMA)	8.6
	JM vacuum (JMV)	10.7
Rough	OptoForce (OF)	4.0
	JM state-switch (JMSS)	6.7
	JM atmospheric (JMA)	5.7
	JM vacuum (JMV)	6.4
Inclined 3°	OptoForce (OF)	3.3
	JM state-switch (JMSS)	5.2
	JM atmospheric (JMA)	2.8
	JM vacuum (JMV)	4.1
Inclined 5°	OptoForce (OF)	1.3
	JM state-switch (JMSS)	3.4
	JM atmospheric (JMA)	0.6
	JM vacuum (JMV)	1.5

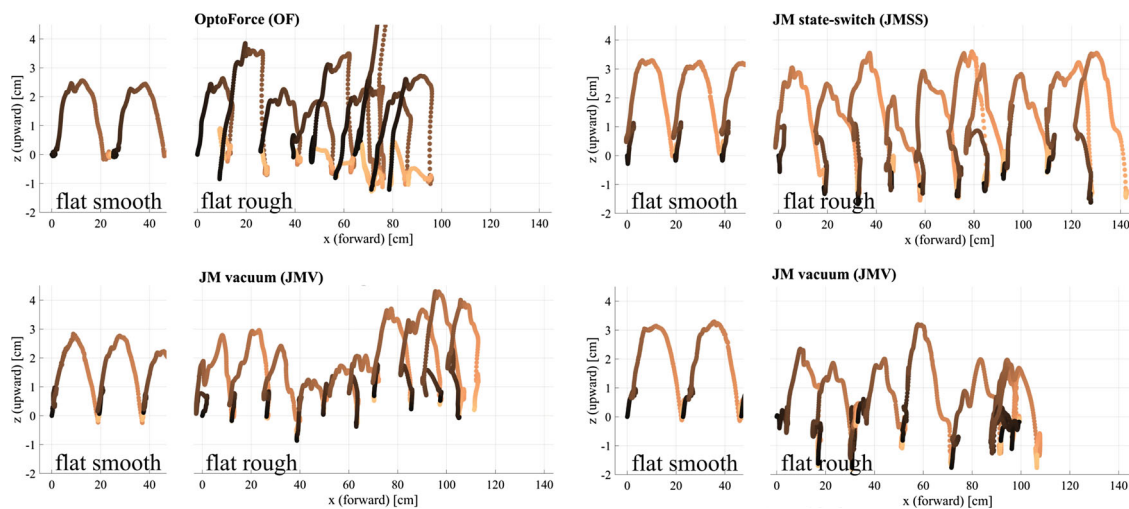


Figure 6. Foot trajectories of the configurations OF, JMSS, JMA and JMV. Each subplot shows approximately 2 gait cycles on flat smooth terrain, followed by 10 gait cycles on flat rough terrain. Each cycle is colored from takeoff (black) to the end of the next stance phase (beige). OF switches to a stochastic, bouncy behavior with non-uniform foot placement when put on rough terrain and a similar transition is visible for JMV, although less pronounced. JMSS and JMA both roughly keep their regular foot placement pattern also on rough terrain due to their superior damping capabilities. A ‘wiggle’ around the contact area formed by the touchdown reduces the average step length of JMA compared to JMSS as part of the leg motion is absorbed by the soft compliance. Due to the state-switch, JMSS is able to use the full propulsion movement of the leg, outperforming the other foot configurations in terms of speed in all the experiments involving rough terrain.

All jamming membranes perform roughly similarly with JMA being the slowest configuration. However, when switching the terrain to the flat, rough case, the speed of the OF sensor feet drastically drops and all jamming membranes locomote faster with the state-switching membrane taking the lead. This tendency gets more pronounced in the inclined terrain cases: the state-switching membrane is considerably faster than any of the other configurations – followed by the full vacuum case – and is even able to climb a 5 degrees inclined terrain where the other foot configurations regularly would get stuck.

The second metric of the tracking data considers the foot tracking and is of more qualitative nature. Figure 6

shows the trajectory of the fore right foot for each foot configuration. In each subplot, approximately two gait cycles of the foot moving on flat, smooth surface is shown. Then, 10 gait cycles of the foot on flat, rough terrain are displayed. Each cycle is colored from takeoff (black) to the end of the next stance phase (beige). The differences in the trajectories on the feet give some insight into the speed metric in Table 1 as the trajectory behavior can vary substantially. In the case of OF, a clean trajectory on smooth terrain can be seen which switches to a rather bouncy and stochastic behavior on rough terrain. The foot placement spacing is not uniform anymore and the robot may even go backward for a short duration,

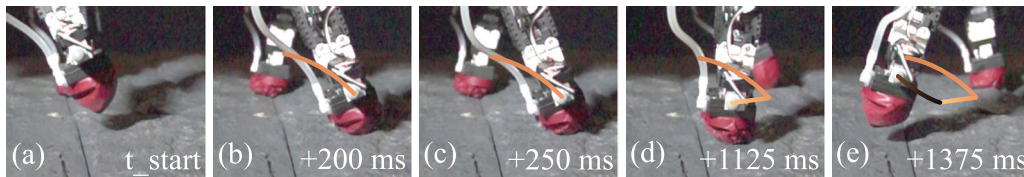


Figure 7. Snapshots of the stance behavior of JMSS. (a) Foot in soft state, approaching touchdown, (b) damping of the impact forces in soft state, (c) state-switch to the hard state in 50 ms, (d) foot in support phase, providing propulsion and (e) state-switch to soft state after takeoff. The tracking of the foot with the approximate color coding as in Figure 6 is indicated.

explaining the sudden loss in performance of this foot from smooth to rough terrain. The jamming membrane under full vacuum has a similar difference in the shapes of the trajectories as the OF case, however less significant. Nevertheless, the higher bounciness compared to JMSS and JMA leads to irregularities in the foot placement, reducing the speed. Both JMSS and JMA are able to keep the trajectory consistent to the smooth ground which is a result of their superior damping capabilities. Their difference lies in the step length. Each step of JMA seems to be slightly shorter than for JMSS due to a ‘wiggling’ around the formed contact area at touchdown and especially at takeoff. The wiggle occurs when part of the motion of the leg is absorbed by the soft compliance instead of generating propulsion, thus slightly reducing the step length. In the case of JMSS, the full propulsion movement of the leg can be used due to the state-switch, resulting in JMSS outperforming the other configurations on all the tested cases involving rough terrain.

The specifics of the discussed effects of jamming membranes are highlighted in the supplementary video where slow motion recordings of selected cases are compared. The video includes the drop tests, a close-up of the state-switching membrane during locomotion, the differences in the touchdown behavior and real-time robot locomotion on different terrains. Snapshots of the stance behavior of JMSS are shown in Figure 7.

5. Conclusion and future work

This work presents an experimental study on the usage of compliant universal grippers as feet for legged locomotion. Universal grippers use the concept of jamming of granular media to switch between two states: a soft, fluid-like state where granules can flow freely, and a hard, solid-like state where the granules are locked in an arrangement. In the context of feet for locomotion, the soft state can provide a damping mechanism that damps the vertical impact forces at touchdown, enabling a faster undisturbed ground contact. Additionally, the soft state allows a passive shape adaptation of the foot to the ground which is especially useful when locomoting on rough terrain. The state-switch can then be used to

harden the foot in this terrain-adapted shape to transmit the horizontal propulsion forces.

We propose a standalone system based on a vacuum pump, a reservoir and valves that is able to quickly and continuously switch the state of jamming membranes as feet. The implementation of the system into a quadruped robotic platform is detailed. The robot consists of a main body and four legs, each formed by two servo motors in series with the jamming membrane as the foot attached. A first validation of the system shows that each foot can separately evacuate to a pressure difference of -500 mbar versus atmospheric pressure in roughly 60 ms, and inflate back to atmospheric pressure in 50 ms. In the used trot gait at 0.5 Hz with a duty factor of 0.5, this corresponds to 6 % and 5 % of the stance and swing duration, respectively. Each foot uses the trigger of a local force feedback from a load cell to switch between states independently, regardless of the state of the other legs. A second series of experiments evolved around the optimal delay between the detection of the trigger and the actual evacuation which was investigated by drop tests of the jamming membranes onto a moving force plate, measuring vertical impact forces and horizontal propulsion forces during and after touchdown. The shortest possible delay was then selected for locomotion experiments both on flat, smooth terrain and flat and inclined rough terrain. It is shown that the superior damping capabilities of the state-switching jamming membrane compared to previously used feet result in a more uniform foot placement pattern even on rough terrain. This enables the robot configuration with state-switching jamming membranes to locomote faster than the other tested configurations on flat rough terrain and even allows the robot to climb steeper inclined terrains with the same open loop control of the foot trajectory.

Currently used feet in legged robots are often simplistic half-spheres of various materials and rarely possess neither stiffness variability nor shape adaptation capabilities which could play a key role in the versatility and locomotion performance of animals. In contrast to contemporary used feet, the unconventional foot design based on the jamming of granular media is a novelty as an attempt to abstract the complex interaction of bones,

muscles and tissues often present in animal feet. It is shown that jamming membranes are able to mimic both the compliance and shape adaptation as well as the stiffness variability. Moreover, the transition between these states through the formation of an interlocked system is not unlike the mechanism in humans created by locking and unlocking the tarsal bones. We regard the preliminary results in this work as a validation of our approach and see much potential in the method of jamming for the application of legged locomotion.

As this is the first prototype of a mobile quadruped with jamming membranes as feet, there are many possibilities of improvement. For experiments on real outdoor terrains, mechanical modifications are needed especially to increase the durability of the membranes. Over the course of the performed experiments, three membranes had to be replaced due to rupture. A real rough terrain is likely to possess more features that can harm the membrane. Although there has been work on different membrane materials [31, 32], in this study we only explored the often used party latex balloons. Further, transferring the system onto a more powerful robotic platform would give insight into the scalability and limitations of the proposed system. This could include dynamic gaits which are not feasible on the used platform. On such a robot, it could be interesting to have the ability to choose the evacuation vacuum pressure – for example based on the gait frequency or ground reaction forces – which would allow a gait-tuned selection of damping and spring characteristics of the foot. In the current system, a foot can only evacuate to a predefined vacuum pressure level in a binary fashion; a more advanced evacuation system would have to be developed. However, the viability of jamming membranes as feet in legged locomotion and their advantages and basic working principles could be demonstrated with this simple system, leaving open many possible directions for further development. Further, jamming membranes can offer the possibility of multi-functional usage as feet, manipulators/grippers and even sensors (e.g. for climbing in [27]).

Disclosure statement

No potential conflict of interest was reported by the authors.

Funding

This project is funded by the Swiss National Science Foundation (Schweizerischer Nationalfonds zur Förderung der Wissenschaftlichen Forschung) (Project 153299) and the Fundação para a Ciência e Tecnologia (FCT) agency of Ministry for Education and Science of Portugal (PD/BD/105781/2014).

Notes on contributors

S. Hauser is a PhD student at the Biorobotics Laboratory (BioRob) at EPFL. He received his MSc in Mechanical Engineering from the Swiss Federal Institute of Technology in Zurich (ETHZ) where his studies were built around bio-inspired robotics. He joined the BioRob in December 2014 where he mainly focuses on modular robotics. His further interests also include evolutionary robotics and soft robotics.

M. Mutlu has a BSc (2011) and MSc (2014) in Electrical and Electronics Engineering from the Middle East Technical University (METU). He is a Ph.D. student in Robotics, Control, and Intelligent Systems (EDRS) and research assistant in Biorobotics Laboratory in EPFL. He is working on the development of modular robots and vision/locomotion-based problems on them.

P. Banzet is a master student at EPFL studying biomechanical and mechanical engineering. He also holds a bachelor degree in mechanical engineering from EPFL. He is currently doing his master thesis at Harvard's Biodesign Lab as a visiting student, and will graduate in October 2018. He is interested in the use of novel technologies such as wearable and soft robotics as well as neuroprosthetics to help physically impaired people regain body functionality.

A. J. Ijspeert is a professor at EPFL, and head of the Biorobotics Laboratory (BioRob). He has Ph.D. in artificial intelligence from the University of Edinburgh and has been at EPFL since 2002, where he was first an SNF assistant professor, then an associate professor (2009), and since 2016 a full professor. His research interests are at the intersection between robotics, computational neuroscience, nonlinear dynamical systems and applied machine learning. He is interested in using numerical simulations and robots to gain a better understanding of animal locomotion and movement control, and in using inspiration from biology to design novel types of robots and locomotion controllers (see for instance, Ijspeert et al., *Science*, Vol. 315, no. 5817, pp. 1416–420, 2007 and Ijspeert, *Science* Vol. 346, no. 6206, 2014). He is also interested in the control of exoskeletons for lower limbs. With his colleagues, he has received paper awards at ICRA2002, CLAWAR2005, IEEE Humanoids 2007, IEEE ROMAN 2014 and CLAWAR 2015. He is member of the Board of Reviewing Editors of *Science* magazine, and associate editor for *Soft Robotics* and for the *International Journal of Humanoid Robotics*.

ORCID

S. Hauser  <http://orcid.org/0000-0002-9502-4587>

M. Mutlu  <http://orcid.org/0000-0003-3666-3159>

A.J. Ijspeert  <http://orcid.org/0000-0003-1417-9980>

References

- [1] Hutter M, Gehring C, Jud D, et al. ANYmal - a highly mobile and dynamic quadrupedal robot. 2016 IEEE/RSJ International Conference on Intelligent Robots and Systems (IROS); Oct; Deajeon, South Korea; 2016 p. 38–44.

- [2] Sprowitz A, Tuleu A, Vespignani M, et al. Towards dynamic trot gait locomotion: design, control, and experiments with Cheetah-cub, a compliant quadruped robot. *Int J Rob Res.* **2013 Jul**;32(8):932–950.
- [3] Poulakakis I, Smith JA, Buehler M. Modeling and experiments of untethered quadrupedal running with a bounding gait: the Scout II robot. *Int J Rob Res.* **2005 Apr**;24(4):239–256.
- [4] Raibert M, Blankespoor K, Nelson G, et al. Bigdog, the rough-terrain quadruped robot. *IFAC Proc Vol.* **2008**;41(2):10822–10825.
- [5] Semini C, Tsagarakis NG, Guglielmino E, et al. Design of HyQ – a hydraulically and electrically actuated quadruped robot. *Proc Inst Mech Eng Part I.* **2011**;225(6):831–839.
- [6] Iida F, Pfeifer R. ‘Cheap’ rapid locomotion of a quadruped robot: self-stabilization of bounding gait. In: Frans Groen, editors. *Intelligent autonomous systems*. Vol. 8. Amsterdam: IOS Press; 2004. p. 642–649.
- [7] Takuma T, Ikeda M, Masuda T. Facilitating multi-modal locomotion in a quadruped robot utilizing passive oscillation of the spine structure. *2010 IEEE/RSJ International Conference on Intelligent Robots and Systems (IROS)*; Oct; Taipei, Taiwan; **2010**. p. 4940–4945.
- [8] Bartsch S, Planthaber S. Scarabaeus: a walking robot applicable to sample return missions. In: Achim Gottscheber, Stefan Enderle, David Obdrzalek, editors. *Research and Education in Robotics - EUROBOT 2008*. Communications in Computer and Information Science. Berlin: Springer; 2008 May. p. 128–133.
- [9] Hong YS, Yi SY, Ryu SB, et al. Design and experimental test of a new robot foot for a quadrupedal jointed-leg type walking robot. *5th IEEE International Workshop on Robot and Human Communication*; 1996 Nov. p. 317–322.
- [10] Kang HJ, Hashimoto K, Kondo H, et al. Realization of biped walking on uneven terrain by new foot mechanism capable of detecting ground surface. *2010 IEEE International Conference on Robotics and Automation (ICRA)*; May; Anchorage, Alaska; **2010**. p. 5167–5172.
- [11] Seo JT, Yi BJ. Modeling and analysis of a biomimetic foot mechanism. *2009 IEEE/RSJ International Conference on Intelligent Robots and Systems (IROS)*; Oct; St. Louis, USA; **2009**. p. 1472–1477.
- [12] Piazza C, Santina CD, Gasparri GM, et al. Toward an adaptive foot for natural walking. *2016 16th IEEE-RAS International Conference on Humanoid Robots (Humanoids 2016)*; Nov; Cancun, Mexico; **2016**. p. 1204–1210.
- [13] Narioka K, Homma T, Hosoda K. Humanlike ankle-foot complex for a biped robot. *2012 12th IEEE-RAS International Conference on Humanoid Robots (Humanoids 2012)*; Nov; Osaka, Japan; **2012**. p. 15–20.
- [14] Fondahl K, Kuehn D, Beinertsdorf F, et al. An adaptive sensor foot for a bipedal and quadrupedal robot. *2012 4th IEEE RAS International Conference on Biomedical Robotics and Biomechanics (BioRob)*; Jun; Rome, Italy; **2012**. p. 270–275.
- [15] Canio GD, Stoyanov S, Larsen JC, et al. A robot leg with compliant tarsus and its neural control for efficient and adaptive locomotion on complex terrains. *Artif Life Rob.* **2016 Sep**;21(3):274–281.
- [16] Abad SA, Sornkarn N, Nanayakkara T. The role of morphological computation of the goat hoof in slip reduction. *2016 IEEE/RSJ International Conference on Intelligent Robots and Systems (IROS)*; Oct; Deajeon, South Korea; **2016**. p. 5599–5605.
- [17] Ohtsuka S, Endo G, Fukushima EF, et al. Development of terrain adaptive sole for multi-legged walking robot. *2010 IEEE/RSJ International Conference on Intelligent Robots and Systems (IROS)*; Oct; Taipei, Taiwan; **2010**. p. 5354–5359.
- [18] kennel club The. 2017. <https://www.thekennelclub.org.uk>.
- [19] Blackwood CB, Yuen TJ, Sangeorzan BJ, et al. The mid-tarsal joint locking mechanism. *Foot Ankle Int.* **2005 Dec**;26(12):1074–1080.
- [20] Donatelli R. Normal biomechanics of the foot and ankle. *J Orthop Sports Phys Ther.* **1985 Nov**;7(3):91–95.
- [21] Liu AJ, Nagel SR. Nonlinear dynamics: jamming is not just cool any more. *Nature.* **1998**;396(6706):21–22.
- [22] Brown E, Rodenberg N, Amend J, et al. Universal robotic gripper based on the jamming of granular material. *Proc Natl Acad Sci.* **2010**;107(44):18809–18814.
- [23] Bajkowski JM, Dyniewicz B, Bajer CI. Damping properties of a beam with vacuum-packed granular damper. *J Sound Vib.* **2015 Apr**;341:74–85.
- [24] Steltz E, Mozeika A, Rodenberg N, et al. JSEL: jamming skin enabled locomotion. *2009 IEEE/RSJ International Conference on Intelligent Robots and Systems (IROS)*; Oct; St. Louis, USA; **2009**. p. 5672–5677.
- [25] Hauser S, Eckert P, Tuleu A, et al. Friction and damping of a compliant foot based on granular jamming for legged robots. *2016 6th IEEE International Conference on Biomedical Robotics and Biomechanics (BioRob)*; Singapore; **2016**. p. 1160–1165.
- [26] Hauser S, Melo K, Mutlu M, et al. Fast state-switching of a jamming-based foot; 2017 Jul. <http://adaptivemotion.org/AMAM2017/files/proceedings/P06.pdf>.
- [27] Hauser S, Mutlu M, Freundler F, et al. Stiffness variability in jamming of compliant granules and a case study application in climbing vertical shafts. *2017 IEEE International Conference on Robotics and Automation (ICRA)*; Brisbane, Australia; **2017**.
- [28] Jiang A, Xynogalas G, Dasgupta P, et al. Design of a variable stiffness flexible manipulator with composite granular jamming and membrane coupling. *2012 IEEE/RSJ International Conference on Intelligent Robots and Systems (IROS)*; Oct; Vilamoura, Portugal; **2012**. p. 2922–2927.
- [29] Amend J, Brown E, Rodenberg N, et al. Positive pressure universal gripper based on the jamming of granular material. *IEEE Trans Rob.* **2012 Apr**;28(2):341–350.
- [30] Vasconcelos R, Hauser S, Dzeladini F, et al. Active stabilization of a stiff quadruped robot using local feedback. *2017 IEEE/RSJ International Conference on Intelligent Robots and Systems (IROS)*; Vancouver, Canada; **2017**. p. 4903–4910.
- [31] Jiang A, Ranzani T, Gerboni G, et al. Robotic granular jamming: does the membrane matter? *Soft Rob.* **2014**;1(3):192–201.
- [32] Amend J, Cheng N, Fakhouri S, et al. Soft robotics commercialization: jamming grippers from research to product. *Soft Rob.* **2016 Dec**;3(4):213–222.